

Interpretation®

Seismic characterization of a blocky mass transport deposit in the Traella Limestone Formation, North Carnarvon Basin, Australia

Journal:	<i>Interpretation</i>
Manuscript ID	INT-2020-0049.R2
Manuscript Type:	2019-08 Interesting Features seen on Seismic Data
Date Submitted by the Author:	30-Jul-2020
Complete List of Authors:	Ortiz Sanguino, Laura; Universidad Industrial de Santander, Escuela de Geología; University of Oklahoma Norman Campus, Geology and Geophysics Tellez, Jerson; University of Oklahoma, Geology and Geophysics Bedle, Heather; University of Oklahoma, School of Geology and Geophysics Martínez-Sánchez, Dilan; Energy and Other Non Renewable Resources Research Group (EONr3g)
Keywords:	seismic geomorphology, seismic attributes, seismic stratigraphy, deepwater, Australia
Subject Areas:	Case studies, Structural, stratigraphic, and sedimentologic interpretation, Amplitudes, attributes, and subsurface properties

SCHOLARONE™
Manuscripts

Seismic characterization of a blocky mass transport deposit in the Traella Limestone Formation, North Carnarvon Basin, Australia

Geological Feature: Glide blocks, North Carnarvon Basin, Australia

Seismic Appearance: Discrete-angular blocks with internal reflectors

Alternative Interpretations: Differential dissolution in a mixed siliciclastic-carbonate environment

Features with similar appearance: Carbonate build ups, differential dissolution blocks

Formation: Trealla Limestone Formation, North Carnarvon Basin

Age: Early-Middle Miocene

Location: Offshore Northwest Australia, North Carnarvon Basin

Seismic data: Obtained from Western Australian Petroleum and Geothermal Information Management System (WAPIMS), Draeck 3D seismic data set.

Contributors: Laura Ortiz-Sanguino^{1,2}, Javier Tellez², Heather Bedle², Dilan Martinez-Sanchez³

Universidad Industrial de Santander, Santander, Colombia

University of Oklahoma, OK, USA

Energy and Other Non Renewable Resources Research Group (EONr3g), Santander,

Colombia

Summary

The deep-water Cenozoic strata in the North Carnarvon Basin, Australia, represent an interval of interest for stratigraphic studies in passive margins settings of mixed siliciclastic-carbonate environments. We explore the geomorphological characteristics of a mass transport deposit (MTD) within the Trealla Limestone Formation to describe in detail the differences among the blocks.

To characterize the individual geometry and structural configuration of the blocks within the MTD, we used geometric seismic attributes such as: coherence, curvature, dip azimuth, and

dip magnitude using horizon slices and vertical profiles. The evaluation shows two types of blocks: remnant and glide (or rafted) blocks. Remnant blocks are in-situ and stratigraphically continuous fragments with the underlying strata. This type of block is frequently fault-bounded and display low deformation evidence. Glide blocks are part of the transported material detached from a paleo-slope. These blocks are deformed and occasionally appear as “floating” fragments embedded within a chaotic matrix in the MTD. Glide blocks are used as kinematic indicators of the direction of deposition of MTD’s.

We illustrate these elements in a modern continental analog that resembles a similar setting for a better understanding of the slide occurrence.

Seismic data

The Draeck 3D seismic survey was acquired in 2007 and covers 2444 km² (29.2 x 83.6km) over the southeastern of the Exmouth Plateau, northwest offshore Australia. The volume contains 1560 inlines and 3346 crosslines with bin size 18.75 m x 25 m. The data is time migrated and has a reverse SEG polarity, which means that a positive change in the acoustic impedance is represented by a trough.

Geological and tectonic background

The tectonic evolution of the North Carnarvon Basin involves several stages of rifting starting on the Late Triassic up to the Late Cretaceous. After this period of extension, during the Cenozoic, the basin became a passive margin where deposition was controlled mainly by relative changes in the sea level.

The Cenozoic strata are characterized by mixed siliciclastic carbonate lithologies with variations in the grain size and composed several geological formations. On seismic, we identified five formations from base to top: the Dockrell, Wilcox, Walcott, Trealla Limestone and Delambre formations. The blocks are interpreted only within the Trealla Limestone Formation. The Miocene deposits of the Trealla Limestone are composed of reworked dolomites and thinly interbedded sandstones. The carbonate composition of the rocks makes this unit prone to produce blocky slide deposits due to its brittle nature.

Geological generalities of blocks related to mass transport deposits

Blocks are common features in MTDs identified nearby to the source areas or at the MTD toe. The blocks are distinguished as a disruption of the seismic reflectors pattern and the preservation of the internal stratigraphy at different degrees of deformation depending on transport magnitude. While remnant blocks are preserved material of the strata where the MTD is deposited, glide blocks are translated laterally from the slide head-scarps to their final position (Gamboa *et al.*, 2011). Glide blocks are irregular but occasionally tend to be rotated in a preferential direction, used as a kinematic indicator of direction of deposition (Gamboa *et al.*, 2011). In a mass transport complex glide and remnant blocks are predominantly located in the middle part of the slide with some few blocks embedded in the debris flow (Figure 1A). Glide blocks are ubiquitous with an expected increase in the deformation down-slope, whereas remnant blocks are more likely located over the proximal areas. The complete extension of the mass transport complex is not observable in the seismic survey (Figure 1B). However, it is likely that head-scarps are eastern outside of the Dreack 3D survey.

We characterize the internal fabric, distribution and structural properties of the blocks to classify the blocks and identify the direction of transport of the MTD.

Methodology

To characterize the MTD setting, we combined geometric attributes such as: coherence, k1 most positive curvature, dip magnitude and dip azimuth. These seismic attribute volumes were computed in the AASPI (Attribute Assisted Seismic Processing and Interpretation) software provided by the University of Oklahoma.

To highlight edges and the convexity of the blocks, we used coherence and k1 most positive curvature respectively. Dip magnitude and dip azimuth as a measure of the direction of maximum dipping and its degree are a good combination for classification of the blocks in terms of their internal strata fabric. We used flattened volumes on the base of the mass transport deposit to provide an integrated plan view of the deposit.

Appearance on seismic data

Blending of coherence and most positive curvature (k1) (Figure 2) displays blocks as individual coherent features with sharp edges, homogeneously distributed and occasionally with a gradational decreasing size from east to west. The most positive curvature (k1) shows positive values highlighting the blocks with a convex morphology or positive relief.

Dip azimuth and magnitude attributes were used for characterization of the deformation since they describe structural variations (direction and magnitude) of strata. In the seismic area, the blocks exhibit two main classes: the First class corresponds to blocks dipping southeast-northwest with average dip azimuth 320° . Class 1 blocks are predominant in the eastern part

of the MTD and exhibit low dip magnitude values ($<6^\circ$). The blocks have an overall east-west orientation and exhibit rounded shapes.

The second class corresponds to blocks dipping southwest to northeast in azimuth range 40° to 75° . The elongated blocks concentrate over the western area with an overall north-south orientation (Figure 3). Class 2 blocks are dipping at relative high angles ($>10^\circ$) and often have internal dip changes (Figure 4).

In the vertical sections (Figure 5), blocks exhibit internal low-amplitude reflections embedded in higher amplitude contorted strata. The contacts between blocks and the surrounding strata display onlap and draping reflections. Overall, blocks preserved the original layering, but their internal fabric is deformed due to transport. Based on the observation of the blocks in vertical sections and horizon slices, we classified and described the blocks within the MTD.

Discussion

The remnant blocks are associated with Class 1 (Figure 3 and 4) and recognized by their minor deformation and sub-planar reflections (Figure 4. Low dipping angles). The stratigraphic and structural continuity with the underlying stratification support that the blocks correspond to in-situ material. Remnant blocks in the seismic area are fault-bounded with subtle faults that also affect the underlying strata (Figure 5A).

On the other hand, glide blocks relate to Class 2. Glide blocks are concentrated over the western part of the data set. They display elongated and irregular shapes and are frequently embedded in contorted strata. The northeastward imbrication of the blocks is evidence of a compressional regime opposite to the direction of deposition (Figure 1. Thrust faulting

dipping contrary to the direction of deposition). Also, this type of blocks can be found “floating” on the chaotic matrix of the MTD (Figure 5). The direction of deposition of the MTD is confirmed in the dip azimuth map (Figure 3) where Class 2 blocks are dipping SW-NE and the dip magnitude map (Figure 4) shows higher angles over the western area, where the imbrications are observed.

The geometry of rafted blocks is generally elongated and dipping eastward direction depending on the intensity of deformation. A general zonation of deformation styles is observed in the direction of deposition where the deformation increases downslope (east to west); although is not perfectly defined and blocks with different deformation degree are often juxtaposed (Figure 5A. and Figure 6. Moderate deformation example). Figure 6 illustrates the different deformation styles: high, moderate and low deformation, following the classification proposed by Gamboa *et al.* (2011). Highly deformed blocks are commonly described over the more distal parts (west) and are tilted at high angles due to intense mobilization and rotation. Moderate deformation corresponds to blocks with changes in their internal dip or folding while low deformed blocks are characterized by nearly horizontal reflections with the same seismic pattern as the underlying strata. Glide blocks increase their deformation while moving down slope and generally are described as high to moderate deformed features; but some low transported blocks can show low deformation.

Based on the attribute horizon slices and the seismic sections, we dismiss the dissolution alternative hypothesis since in the curvature sections evidence paleo tops in the center of the features instead of depressions. Similarly, the sections support that the features were deposited previously to the surrounding strata due to the terminations over the blocks previously described.

Modern analog

Modern analogs in continental settings are often used to describe MTD's despite their genetic differences. The Toreva block landslide (Figure 7) displays slide blocks located at the Hopi-Indian Reservation of the Northeastern Arizona below the Echo Cliffs and was first described by Parry Reiche in 1937 who identified a distinctive triggering mechanism. A Toreva block landslide occurs when a stronger rock-type such as sandstone or limestone overlies a weaker material such as shale and an eroding agent undercuts the weaker lower layer. It is also characteristic to exhibit a backward rotation toward the parent cliff. However, some remnant blocks over the area that correspond to underlying strata that were not eroded by the landslide.

In the satellite image, it is noticeable that the internal stratigraphy of the blocks remains preserved as described in the seismic, even though the genesis conditions differ due to the media where was originated. However, contrary to the Toreva block, the triggering mechanism for the glide blocks deposit is hard to be determinate since the head-scarps are located outside the seismic survey, then the original setting where the slide was generated is unknown.

Conclusion

This case study showed an application of the geometric seismic attributes for the characterization of blocky mass transport deposits. We demonstrated that by integrating the observations of modern analogs and schematic models with seismic attributes is possible to infer the direction of deposition even in settings where no other kinematic indicators such as head-scarps are evident. In this MTD example, we used the block deformation as criteria for

1
2
3 the classification and used the dominant dipping direction to deduce the source location of
4 the deposit.

5 6 7 8 9 10 11 12 13 **Acknowledgements**

14 We want to thank the Western Australian Petroleum and Geothermal Information
15 Management System (WAPIMS) for releasing the data used in this study. To Schlumberger
16 for their kind donation of Petrel 2019 for developing the seismic interpretation. Also, to
17 AASPI consortium for providing licenses for attribute analysis. Special thanks to our
18 Interpretation reviewers for their feedback throughout the revision process.

19 20 21 22 23 24 25 **References**

26 Gamboa, D., T. Alves, and J. Cartwright, 2011, Distribution and characterization of failed
27 (mega)blocks along salt ridges, southeast Brazil: Implications for vertical fluid flow on
28 continental margins: *Journal of Geophysical Research Atmosphere*, **116**, no. B08103, doi:
29 10.1029/2011JB008357.

30 Kneller, B., M. Dykstra, L. Fairweather and J.P. Milana, 2016, Mass-transport and slope
31 accommodation: Implications for turbidite sandstone reservoirs: *AAPG Bulletin*, **100**, no. 2,
32 213–235, doi: 10.1306/09011514210.

33 Chopra, S., and K. J. Marfurt, 2007, Seismic attributes for prospect identification and
34 reservoir characterization: *Society of Exploration Geophysicists*.

35 Martinez, F. J., 2010, 3D seismic interpretation of mass transport deposits: Implications for
36 basin analysis and geohazard evaluation, *in* D. C. Mosher, C. Shipp, L. Moscardelli, J.
37 Chaytor, C. Baxter, H. Lee, and R. Urgeles, eds., *Submarine mass movements and their*
38 *consequences. Advances in natural and technological hazards research: Springer* 553–568.

1
2
3 Prince, P.S., 2019, Toreva Block landslide models,
4 <https://geomodelsvt.wordpress.com/2019/07/29/toreva-block-landslide-models/>, accessed 7
5 January 2020.

6
7 Reiche, P., 1937, The Toreva-block: A distinctive landslide type: *Journal of Geology*, **45**, no.
8 5, 538–548, doi: 10.1086/624563.

9
10 Weimer, P., and R.M. Slatt, 2007, Introduction to the petroleum geology of deepwater
11 settings: AAPG Studies in Geology.

12
13
14
15
16
17
18
19
20
21
22
23
24
25
26
27
28
29
30
31
32
33
34
35
36
37
38
39
40
41
42
43
44
45
46
47
48
49
50
51
52
53
54
55
56
57
58
59
60

1
2
3 Figure 1. A. Schematic figure of the mass transport facies showing the two classes of blocks:
4 remnant, found in situ and glide blocks, translated downward from the head-scarps to their
5 current position. Note that remnant blocks are frequently found over the proximal area while
6 glide blocks are more ubiquitous with an increasing internal deformation down-slope with a
7 compressional regime in the distal part of the slide. Modified after Kneller *et al.* (2016). B.
8 Coherence horizon slice (~1804 ms) of the MTD facies in the Traella Limestone where
9 discrete blocks (remnant and glide) are distinguishable over the northeastern area of the
10 seismic dataset but west-ward the chaotic material predominates.

11
12
13
14
15
16
17
18
19
20
21
22
23
24
25
26
27
28
29
30
31
32
33
34
35
36
37
38
39
40
41
42
43
44
45
46
47
48
49
50
51
52
53
54
55
56
57
58
59
60
Figure 2. A. Location map of the Draeck 3D seismic survey at the northwest offshore
Australia (Modified from Google Earth 2020) B. Coherence and K1 curvature blending
extracted over horizon slice (base of the Traella Limestone) at 1804 ms. Note that the edges
of the blocks are marked by low coherence values but internally are highly coherent. K1 most
positive curvature shows positive values within the features suggesting a convex
morphology. Some of the best-defined blocks by k1 most positive curvature are shown in
Figure 2C.

Figure 3. A. Coherence and dip azimuth blending on horizon slice (base of the Traella
Limestone) at 1804 ms. The dip azimuth attribute shows two clusters of blocks: the first class
corresponds to the green-blue blocks which are dipping SE-NW (~320°) and are concentrated
over the eastern sector. The second class are blocks dipping SW-NE (40-75°), color coded
with pink purple; and are mainly localized over the western area of the MTD. However, none

of the classes are restricted to a particular area and different class blocks can be contiguous. Figure B and C are detailed images of some blocks evidencing the two trends; white arrows are pointing Class 1 blocks (remnant) and the yellow ones point good examples of glide blocks.

Figure 4. A. Coherence and dip magnitude blending extracted on horizon slice (base of the Traella Limestone). The dip magnitude attribute horizon slice evidences that most of the blocks over the eastern area, named as Class 1 (Figure 3), are dipping at low angles ($<6^\circ$) with some high values at the edges. Over the western area dip magnitude increases showing a predominant range of ($10-12^\circ$) in the blocks of Class 1. Also, some blocks have internal changes in dip suggesting folding (e.g. Fig. 4B. Yellow arrow 1). Figures 4B. and 4C. are zoomed figures exhibiting the described trend.

Figure 5. Seismic amplitude sections illustrating the two dipping trends showed in Figure 3. Seismic section (A) evidence some highly deformed blocks dipping steeply east ward and also floating blocks over the distal area. (B) Evidences that over the eastern area the blocks follow the dip of the gliding surface and their internal stratification is well-preserved and continuous; suggesting in situ fragments (remnant). Also, note the fault-bounding in some of the remnant blocks. The deformation increases west-ward indicated by the imbrications opposite to that direction and some blocks remain “floating” over the chaotic matrix. **Rafted blocks are delimited by the green line while remnant blocks are highlighted in purple.**

1
2
3 Figure 6. Examples of blocks with different deformation degrees. Location of the blocks is
4 shown on Figure 2B. Glide blocks are described as moderate to highly deformed features
5 while remnant blocks exhibit minor deformation. Highly deformed blocks (A) are dipping
6 $>15^\circ$ towards the SE; note that this type of block is often in contact with subhorizontal blocks;
7 meaning that deformation is not a defined zonation. Moderate deformed blocks (B) show
8 some internal changes in dip recognized by subtle folding. Low deformed blocks (C) have
9 the same seismic pattern of the underlying strata, being essentially subhorizontal.

10
11
12
13 Figure 7. Satellite image of a Toreva Block Landslide nearby Toreva, Arizona. The blocks
14 are characterized by preserving the internal layering and a considerable extension up to 2000
15 ft. Note the rotation of the blocks towards the source area in the glide blocks and the nearly
16 horizontal dip on the remnant blocks. The triggering mechanism corresponds to a distinctive
17 intercalation of a hard material overlying a soft rock type. Retrieved from Google Earth
18 ($36^\circ 36' 20.18''$ N; $111^\circ 38' 50.77''$ W).

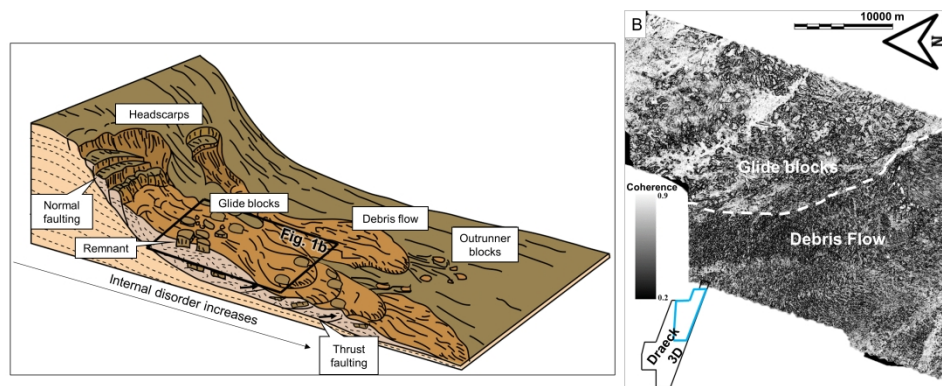


Figure 1. A. Schematic figure of the mass transport facies showing the two classes of blocks: remnant, found in situ and glide blocks, translated downward from the head-scarps to their current position. Note that remnant blocks are frequently found over the proximal area while glide blocks are more ubiquitous with an increasing internal deformation down-slope with a compressional regime in the distal part of the slide. Modified after Kneller et al. (2016). B. Coherence horizon slice (~ 1804 ms) of the MTD facies in the Traella Limestone where discrete blocks (remnant and glide) are distinguishable over the northeastern area of the seismic dataset but west-ward the chaotic material predominates.

376x167mm (300 x 300 DPI)

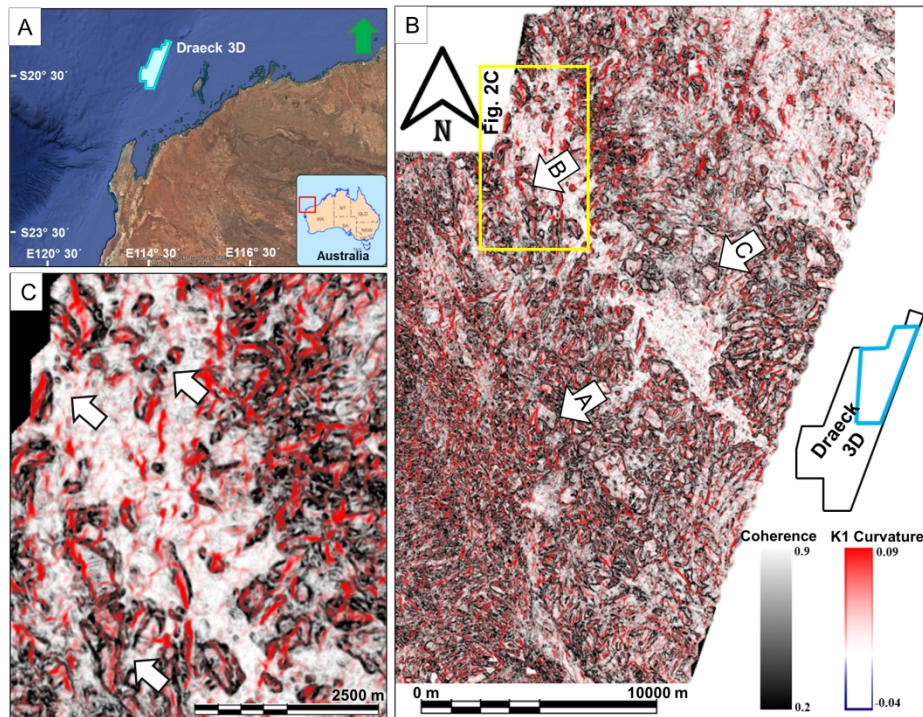


Figure 2. A. Location map of the Draeck 3D seismic survey at the northwest offshore Australia (Modified from Google Earth 2020) B. Coherence and K1 curvature blending extracted over horizon slice (base of the Traella Limestone) at 1804 ms. Note that the edges of the blocks are marked by low coherence values but internally are highly coherent. K1 most positive curvature shows positive values within the features suggesting a convex morphology. Some of the best-defined blocks by k1 most positive curvature are shown in Figure 2C.

250x186mm (300 x 300 DPI)

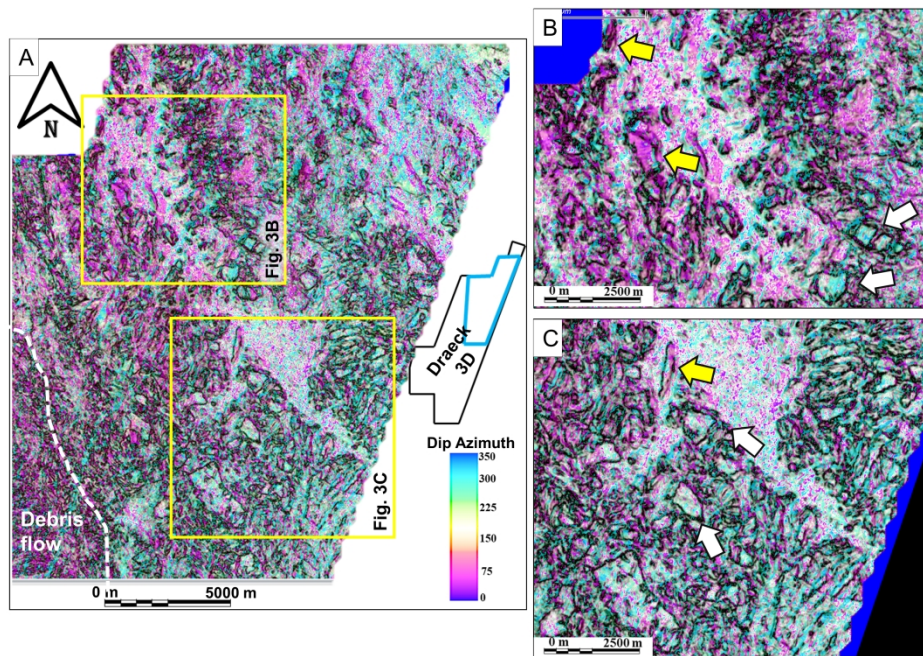


Figure 3. A. Coherence and dip azimuth blending on horizon slice (base of the Traella Limestone) at 1804 ms. The dip azimuth attribute shows two clusters of blocks: the first class corresponds to the green-blue blocks which are dipping SE-NW ($\sim 320^\circ$) and are concentrated over the eastern sector. The second class are blocks dipping SW-NE ($40\text{--}75^\circ$), color coded with pink purple; and are mainly localized over the western area of the MTD. However, none of the classes are restricted to a particular area and different class blocks can be contiguous. Figure B and C are detailed images of some blocks evidencing the two trends; white arrows are pointing Class 1 blocks (remnant) and the yellow ones point good examples of glide blocks.

275x187mm (300 x 300 DPI)

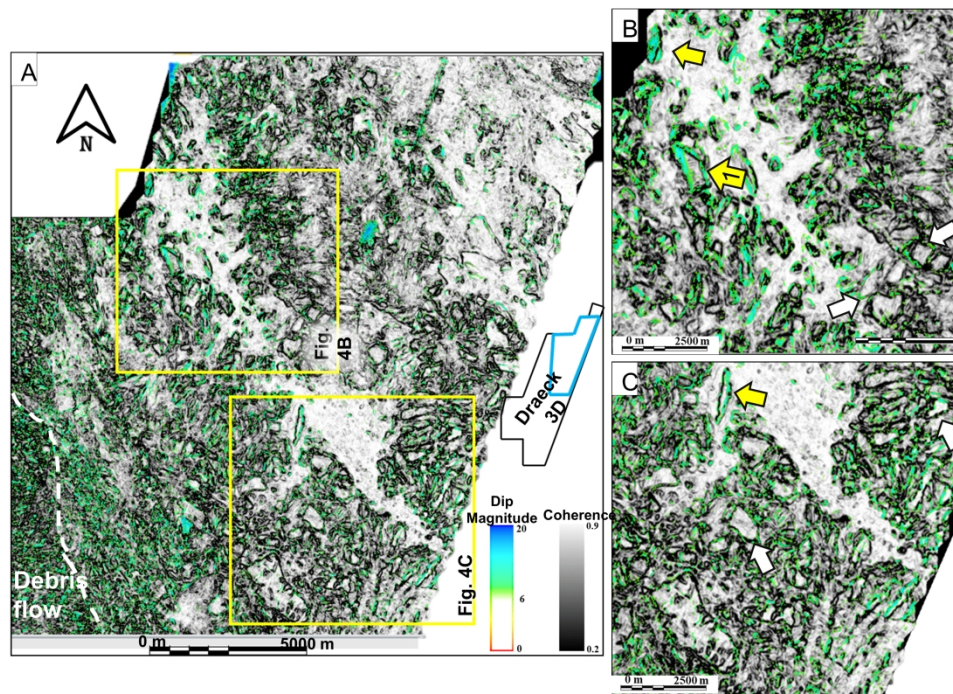


Figure 4. A. Coherence and dip magnitude blending extracted on horizon slice (base of the Traella Limestone). The dip magnitude attribute horizon slice evidences that most of the blocks over the eastern area, named as Class 1 (Figure 3), are dipping at low angles ($<6^\circ$) with some high values at the edges. Over the western area dip magnitude increases showing a predominant range of ($10\text{--}12^\circ$) in the blocks of Class 1. Also, some blocks have internal changes in dip suggesting folding (e.g. Fig. 4B. Yellow arrow 1). Figures 4B. and 4C. are zoomed figures exhibiting the described trend.

261x188mm (300 x 300 DPI)

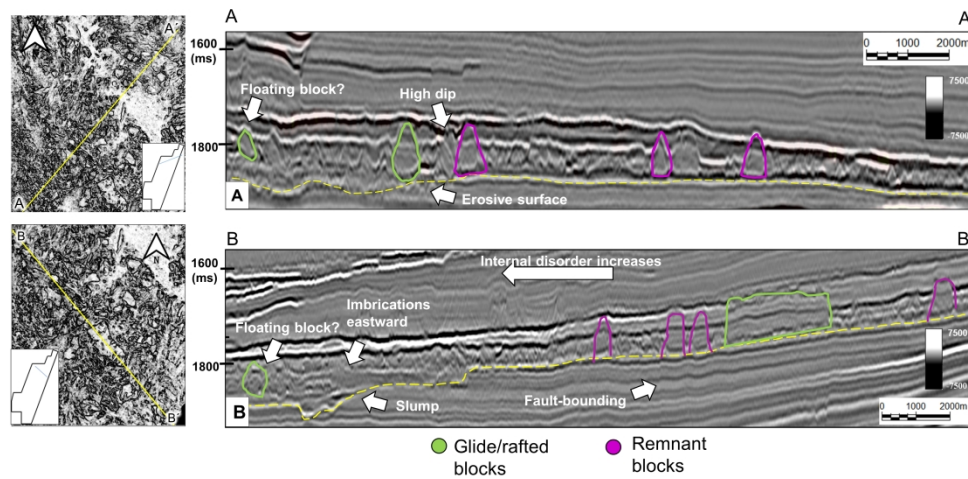


Figure 5. Seismic amplitude sections illustrating the two dipping trends showed in Figure 3. Seismic section (A) evidence some highly deformed blocks dipping steeply east ward and also floating blocks over the distal area. (B) Evidences that over the eastern area the blocks follow the dip of the gliding surface and their internal stratification is well-preserved and continuous; suggesting in situ fragments (remnant). Also, note the fault-bounding in some of the remnant blocks. The deformation increases west-ward indicated by the imbrications opposite to that direction and some blocks remain "floating" over the chaotic matrix. Rafted blocks are delimited by the green line while remnant blocks are highlighted in purple.

346x171mm (300 x 300 DPI)

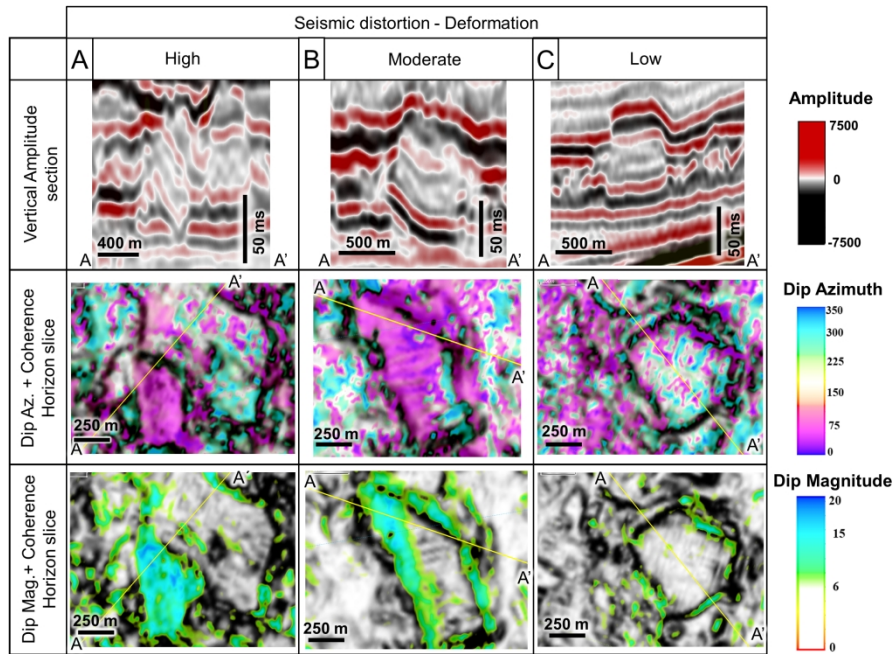


Figure 6. Examples of blocks with different deformation degrees. Location of the blocks is shown on Figure 2B. Glide blocks are described as moderate to highly deformed features while remnant blocks exhibit minor deformation. Highly deformed blocks (A) are dipping $>15^\circ$ towards the SE; note that this type of block is often in contact with subhorizontal blocks; meaning that deformation is not a defined zonation. Moderate deformed blocks (B) show some internal changes in dip recognized by subtle folding. Low deformed blocks (C) have the same seismic pattern of the underlying strata, being essentially subhorizontal.

244x174mm (300 x 300 DPI)



Figure 7. Satellite image of a Toreva Block Landslide nearby Toreva, Arizona. The blocks are characterized by preserving the internal layering and a considerable extension up to 2000 ft. Note the rotation of the blocks towards the source area in the glide blocks and the nearly horizontal dip on the remnant blocks. The triggering mechanism corresponds to a distinctive intercalation of a hard material overlying a soft rock type. Retrieved from Google Earth (36°36'20.18' N; 111°38'50.77' W).

203x119mm (300 x 300 DPI)

DATA AND MATERIALS AVAILABILITY

Data associated with this research are available and can be obtained by contacting the corresponding author.